8-1-2017

Eye Repair in Xenopus Laevis

Cindy Xuan-Mai Kha
University of Nevada, Las Vegas

EYE REPAIR IN *XENOPUS LAEVIS*

By

Cindy Xuan-Mai Kha

Bachelor of Science – Neuroscience
University of California, Riverside
2010

Master of Science – Biology
California State University, Los Angeles
2014

A thesis submitted in partial fulfillment
of the requirements for the

Master of Science - Biological Sciences

School of Life Sciences
College of Sciences
The Graduate College

University of Nevada, Las Vegas
August 2017

UNLV | GRADUATE COLLEGE

Thesis Approval

The Graduate College
The University of Nevada, Las Vegas

April 5, 2017

This thesis prepared by

Cindy Xuan-Mai Kha

entitled

EYE REPAIR IN *XENOPUS LAEVIS*

is approved in partial fulfillment of the requirements for the degree of

Master of Science - Biological Sciences
School of Life Sciences

Ai-Sun Tseng, Ph.D.
Examination Committee Chair

Kathryn Hausbeck Korgan, Ph.D.
Graduate College Interim Dean

Andrew Andres, Ph.D.
Examination Committee Member

Nora Caberoy, Ph.D.
Examination Committee Member

Allen Gibbs, Ph.D.
Examination Committee Member

Hong Sun, Ph.D.
Graduate College Faculty Representative

ABSTRACT

EYE REPAIR IN *XENOPUS LAEVIS*

By

Cindy Xuan-Mai Kha

Ai-Sun Tseng, PhD, Committee Chair
Assistant Professor of Biology
University of Nevada, Las Vegas

Eye development in vertebrates of complex steps that include specific interactions of the neuroectoderm and overlying head ectoderm. The African clawed frog, *Xenopus laevis* (*X. laevis)*, has a well-characterize eye developmental pathway and is an established model for eye regeneration research. Additionally, *Xenopus* frogs have high regenerative abilities to regenerate individual eye tissues such as the retina, lens, and cornea. However, it was previously shown that the removal of the specified eye field during the neurulation stage or an eye during the swimming tadpole stage does not permit an eye to regenerate. Here we will describe a model for investigating eye regeneration. We discovered that eye regrowth occurs in tailbud embryos after the surgical removal of the specified optic vesicle tissues. Regrown eyes are found to show similar morphology and reach similar size to a contralateral, internal control eye by 5 days of recovery. Additionally, the regrown eye has expected eye structures, including all cell types of the retina and the lens. Furthermore, we found that eye regrowth requires an early bioelectrical signaling mechanism as seen in appendage regeneration. Overall, our results indicate that *Xenopus* tailbud embryos can regenerate an eye after tissue lost through a process that requires a known mechanism driving regeneration.

TABLE OF CONTENTS

LIST OF FIGURES

CHAPTER 1

INTRODUCTION

Regeneration is the ability to repair injuries and restore the morphology and functional integrity of tissues and organs. A range of animals display the capacity for tissue regeneration, including amphibians and planarians as first described in 1768 from regeneration and transplantation experiments by the physiologist, Lazzaro Spallanzani (Spallanzani, 1768). Even as adults, the urodele amphibian, newts can generate their tails, limbs, and ocular tissues (Oberpriller and Oberpriller, 1974; Eguchi et al., 2011). Additionally, the anuran amphibian, *X. laevis* can regenerate tails and limbs (Beck et al., 2003; Lin et al., 2013). The impressive regenerative abilities in these species have contributed significantly to our understanding of the complex process of regeneration and have led to important questions in research. What are the mechanisms involved to signal and drive the regeneration process and where the location(s) of new source cells is/are from? Previous research to understand the mechanisms and cellular source(s) in amphibians can help understand how some organisms can respond to repair injuries for their survival with the goal in regenerative medicine to improve wound healing and regeneration in humans. The ability to do research in amphibians with high capabilities to regenerate can provide valuable information for efficient tissue repair and contribute to regeneration therapies.

One vertebrate with high regenerative capability is the African clawed frog, *Xenopus laevis*. *Xenopus* frogs have the advantage of being a well-studied laboratory model organism and have regenerative abilities seen in tadpole tail regeneration (Beck et al., 2003), gut epithelium

regeneration (McAvoy and Dixon, 1977), and eye lens regeneration (Freeman, 1963; Reeve and Wild, 1978).

Xenopus laevis, is one of the most well studied in vertebrate embryology and well used in developmental biology. The female frogs can be induced to produce embryos in any season, making it possible to obtain embryos year-round (Parker Jr. et al., 1947). Embryos are easily obtained, the large size makes it easy to perform surgical manipulation at any developmental stage, and the ease of injecting a range of materials (e.g. nucleic acids or proteins) into the embryos have contributed to the discovery of many genes with key functions in development. Furthermore, the genome has been sequenced (Session, 2016). More recently, *X. laevis* has been established as a model for eye development and regeneration studies (Vergara and Rio-Tsonis, 2009). The *X. laevis* eye model is a useful tool as the frog eye is similar to humans showing shared structures and development with only differences in development time (Zuber, 2010) **(Figure 1)**.

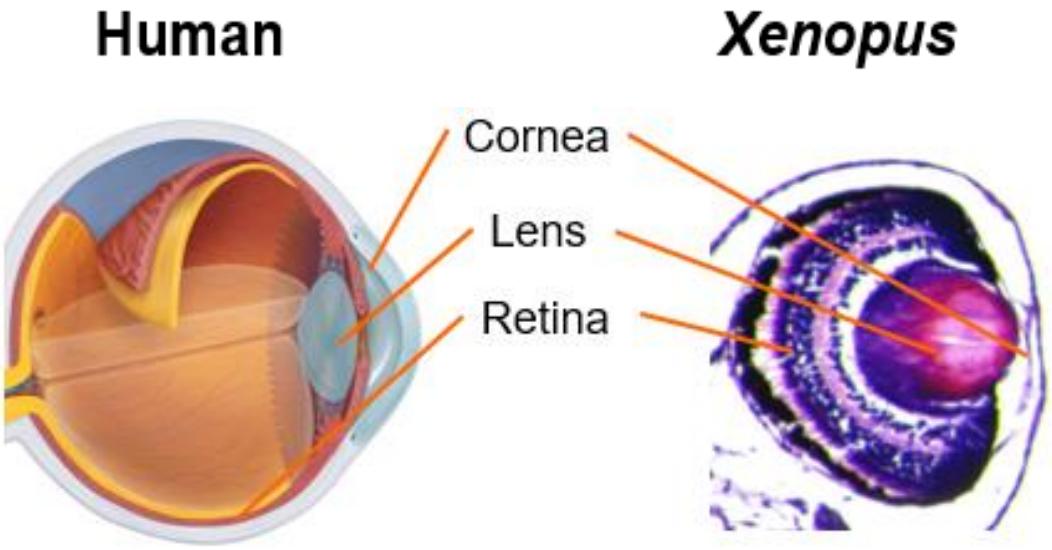

Figure 1. *Xenopus* eye is similar to humans. *Xenopus* eye phenotype has structures similar to the human eye such as the transparent cornea in the front of the eye, the lens, and the retinal layer leading to the back of the eye. Orange lines: show similarities between the *Xenopus* and human eyes (image of the human eye adapted from Pearson Education, Inc. 2010).

OVERVIEW OF *XENOPUS* EYE DEVELOPMENT

The *Xenopus* eye has many of the same structures found in a vertebrate eye such as the outermost cornea, the transparent lens, and the retina. Similar to vertebrate eye development, the *Xenopus* eye requires a series of complex steps that include specific inductive signals to the anterior neural plate to form structures necessary for future eye development. The steps for *Xenopus* eye development are compose of a series of retinal cellular differentiation to form the retina and the differentiation of lens cells to form the lens (Chow and Lang, 2001).

During early eye development, the interaction of the neuroectoderm and overlying head ectoderm induces a series of events to form the complex eye structures. During neurulation at development stage (st.) 15, the eye field or tissues that are specified to form future eye tissues are present with expression of numerous transcription factors known as the eye field transcription factors (EFTFs; Zuber et al., 2003). By early tailbud embryo at development st. 22, the invagination of the neuroectoderm forms the distinctive optic vesicles (an outgrowth of the neural tube) and part of the head ectoderm thickens by cell elongation and forms the lens placode. Lens specification is established as the optic vesicle interacts with the head ectoderm (Henry and Grainger, 1990). Further through development at the late tailbud embryo development st. 27, the optic vesicle further invaginates to form the double layered optic cup, with the inner cup forming the neural retina tissue and outer layer forming the future retina pigmented epithelium (RPE). The invagination of the lens placode will give rise to the lens vesicle. Both the invagination of the optic vesicle and lens placode is in tandem (Henry and Grainger, 1990).

In the retina, there are seven distinctive cell types **(Figure 1)**. The layer of the retina closest to the lens is the ganglion cell layer (GCL) that houses the retinal ganglion cells (RGC)

and some amacrine cells. The next layer is the inner nuclear layer (INL) which contains bipolar, more amacrine, and horizontal cells. The outer nuclear layer (ONL) contains the rods and cones photoreceptors. In additional, Müller glial cells span the entire retina from the GCL to the photoreceptor cell bodies. Furthermore, the retinal pigment epithelium (RPE) is located at the outermost layer of the retina and the choroid (vasculature of the eye).

The process of retinal development has been extensively studied in *Xenopus* frogs. Retinal cells are generated from multipotent retinal progenitor cells (RPCs) in early eye development. The RPCs are from the double layered optic cup and are located in the inner most layer of the retina (Wetts and Fraser, 1988). In later eye development after the mature retina has been formed throughout the life of the tadpole to an adult frog, the *Xenopus* retina continues to grow and increase in size by adding new cells of all retinal type (Hollyfield, 1971; Reh, 1989; Wetts et al., 1989). This area of cell growth and differentiation is located at the peripheral of retina called the ciliary marginal zone (CMZ) and is spatially organized by level of differentiation. The youngest and less differentiated stem cells are located close to the periphery of the CMZ at the distal tip, the more differentiated retinal progenitor cells are in the central portion of the CMZ, and post mitotic cells that have stop dividing and are further along in the process of differentiating are located at the opposite edge. The presence of structures that have retinal stem cells in *Xenopus* could be a major potential cell source for regeneration studies as mammals do not generally show evidence of proliferation at the peripheral edge of the normal retina (Araki, 2014).

RETINAL REGENERATION

The *Xenopus* frog can regenerate individual eye tissues such as the neural retina at both tadpole and adult stages through the transdifferentitation of the RPE. The process of RPE transdifferentitation can be seen with various manipulations including, chemical ablation (Choi et al., 2011), genetic ablation (Martinez-De Luna et al., 2011), and surgical removal of tissues (Ide et al., 1988; Vergara and Del Rio-Tsonis, 2009). Also, adult frogs can repair multiple cell types in the retina (Yoshii et al., 2007).

In previous research, it was shown that when the retina was surgical removed from a post-metamorphic *Xenopus* frog, leaving behind the RPE and CMZ, the retina can partially regenerate from the proliferating cells in the CMZ (Mitashov and Maliovanova, 1982). From this, the tissues that remain can be potential sources of cells for repair in the retina. Recently, a study in post-metamorphic frogs following retina removal, leaving the RPE and vascular membrane behind, demonstrated the ability of the RPE cells to migrate and attached to the vascular membrane to transdifferentiate into neural retina (Yoshii et al., 2007). Additionally, another model system for retinal regeneration was described showing *X. laevis* tadpoles can regenerate a retina after complete surgical removal through the transdifferentitation of the RPE in the presence of fibroblast growth factor 2 (FGF2) (Vergara and Rio-Tsonis et al., 2009). Furthermore, in the zebrafish, Müller glia cells can regenerate all cell types after damage to the retina (Wan and Goldman, 2016). In *Xenopus*, Müller glia cells re-enter the cell cycle after damage to the retina (Hidalgo et al., 2014).

LENS REGENERATION

Xenopus tadpoles can regenerate the lens can from the cornea epithelium following lentectomy surgery (Freeman, 1963). However, wounding of the outer cornea fails to initiate

lens regeneration. Only after cornea cells are transplanted back into the eye can a lens regenerate from the transdifferentitation of the cornea cells through a series of distinctive steps (Freeman, 1963). Until now, research to understand the mechanisms driving cornea to lens regeneration has been on tadpole stages as the ability of the cornea epithelium to give rise to a new lens was reported to be progressively lost after metamorphosis (Freeman, 1963; Filoni et al., 2009). However, recent research show post-metamorphosis frogs can regenerate lens after lentectomy from the mature cornea even with missing retina tissue (Yoshii et al., 2007).

EYE REPAIR

Xenopus laevis provides numerous advantages for use as an animal model for eye research, such as the similarities to a human eye **(Figure 1),** fast development, and well-known eye development pathway. Additionally, it is a well-established as a model for eye studies of single-tissue repair (Beck et al., 2009; Martinez-De Luna et al., 2011). One interesting question from these studies that can be asked is if the tadpole lost more eye tissues, would repair still occur? However, this question was previously addressed when the eye field was removed during the neurulation stage of an embryo and no eye repair was seen (Zuber, 2010). Furthermore, removal of an eye during the swimming tadpole stage shows no regrowth of the eye following surgery and recovery (Blackiston and Levin, 2013).

Preliminary results from the Tseng lab show that an eye can regrow after eye tissue removal from the tailbud embryo stage. To establish this new model, our immediate goal is to characterize the regrown eye and compare it to a normally developing eye with three aims:

Aim 1: Assess if the regrown eye is similar to a normal eye.

Aim 2: Define the order of events during eye regrowth.

Aim 3: Address the mechanism used in eye regrowth.

We can further our understanding of the regeneration process in animal models that have the capability to regenerate eye structures from this research. Our long-term goal is to apply what is known from our results to other organisms, including humans. This could have significant implications in the development of regenerative therapies for eye related diseases.

CHAPTER 2

MATERIALS AND METHODS

EMBRYO CULTURE

Xenopus laevis adult frogs were obtained from Nasco (Janesville, WI). Embryos were fertilized *in vitro* and raised in 0.1X Marc's Modified Ringer's (MMR; 10Mm NaCl, 2.0 Mm KCl, 1 Mm $MgSO_4$, 2 Mm $CaCl_2$, 5 Mm HEPES, Ph 7.8) solution (Sive et al., 2000). Embryos were grown in petri dishes containing 0.1X MMR at 14-22°C. All protocols and procedures were approved by the University of Nevada, Las Vegas Institutional Animal Care and Use Committee.

EYE REGENERATION ASSAY

Xenopus laevis tailbud embryos at developmental stage (st.) 27 were selected according to Nieuwkoop and Faber, 1994, and anesthetized in 0.05% tricaine methanesulfonate (MP Biomedicals). The left optic vesicle tissue was removed using Dumont No.5 forceps under a dissecting microscope. Following surgery, all animals were washed in 0.1X MMR twice and transferred to new 0.1X MMR and cultured at 22°C in petri dishes for 5 days and scored for eye regrowth. A scoring method called the regeneration index (RI) was introduced to compare the regrowth efficiency of a regrown eye compared to a control eye. Each regrown eye was assigned into one of four phenotype categories for scoring **(Figure 2A-D)**:

- full, regeneration of an eye comparable to an unoperated control eye **(Figure 2A)**

- partial, misshapen and reduction in eye size (incomplete closure of the choroid fissure; **Figure 2B**)
- weak, no lens and severely malformed eye with most tissues missing (failure of eye development and retinal pigmentation; **Figure 2C**)
- none, no regenerated tissues (**Figure 2D)**

Based on the calculation of the percentage of the number of individuals grouped to each category, each category is then multiplied by 3 (full), 2 (partial), 1 (weak), or 0 (none). The resulting number is a value ranging from 0 to 300, constituting the RI. A value of 0 denotes no regeneration in any of the individuals, while a value of 300 denotes full regeneration in 100% of individuals in a dish.

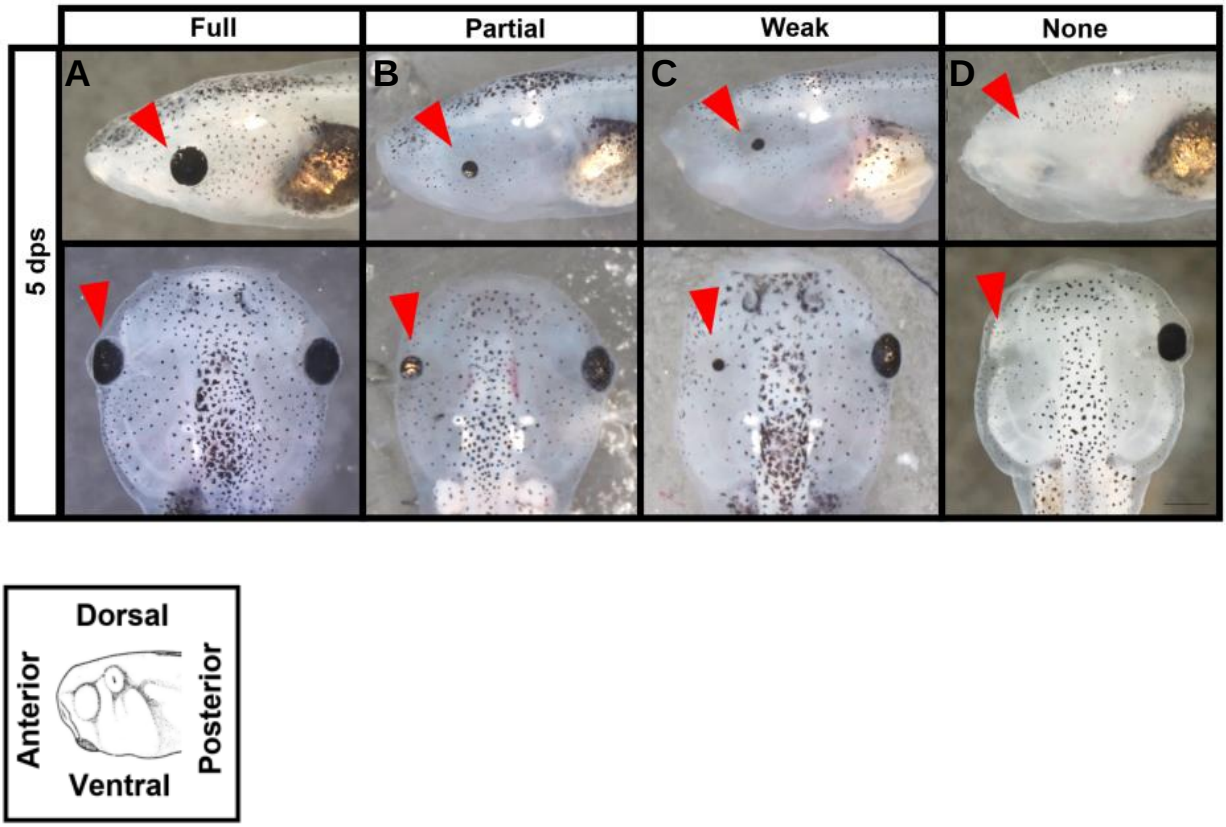

Figure 2. Eye regeneration efficiency based on four phenotype categories. For comparison of regeneration efficiency in regenerated eye versus the control eye, a scoring method called the regeneration index (RI) was introduced to compare individuals in each dish. Eye regeneration efficiency was scored based on four phenotype categories after 5 days post-surgery (dps). **(A)** Full, show regeneration of an eye comparable to unoperated control eye. **(B)** Partial, reduction eye size and misshapen eyes such as the incomplete closure of the choroid fissure. **(C)** Weak, no lens developed and severe malformed eye with most tissues missing including the failure of eye development and retinal pigmentation. **(D)** None, no eye tissues regenerated. Closed arrowheads: surgical eye. Scalebar=500 µm.

EYE TRANSPLANTATION ASSAY

Tailbud embryos at st. 27 had the left optic vesicle was removed with #5 forceps. The removed tissue was grafted back on to the same animal in a small incision made at the posterior end along the body axis as previously described (Blackiston and Levin, 2013). Following surgery, all animals were washed in 0.1X MMR twice and transferred to new 0.1X MMR and cultured at 22°C in petri dishes for 5 days and scored for eye regrowth.

INHIBITOR CHEMICAL ASSAY

Chemical exposure for the loss-of-function experiment was performed with a potent and highly-specific V-ATPase inhibitor concanamycin (Woo et al., 1996) at a concentration of 20 nM. Stocks were made in Dimethyl sulfoxide (DMSO) at 100 µM/mL. Immediately after optic vesicle surgery, animals were exposed to the inhibitor within 5 minutes for 24 hours. To stop exposure, animals were washed in 0.1X MMR twice and transferred to new 0.1X MMR and cultured at 22°C in petri dishes until 5 days after surgery and scored for eye regrowth.

TISSUE PROCESSING AND STAINING

Tailbud embryos and tadpoles were fixed overnight in MEMFA (100 mM MOPS pH 7.4, 2 mM EGTA, 1 mM $MgSO_4$, 3.7%(v/v) formaldehyde) solution (Sive et al., 2000). After fixation, animals were washed twice in 1X phosphate-buffered saline (PBS), and dehydrated in a graded ethanol series and embedded in Paraplast X-TRA to be sectioned with a Tissue-Tek Accu-Cut Rotary Microtome. In addition, fixed animals were cryoprotected in 20% sucrose and embedded in optimum cutting temperature (O.C.T.) solution to be sectioned with an UltraPro 5000 Cryostat. Alternatively, fixed animals were embedded in 1% low melting point agarose to

be sectioned with Leica VT1000 S Vibratome. For histological stains, 10 µm paraffin sections were stained with Hematoxylin and Eosin (H&E). For immunofluorescence stains, either paraffin, O.C.T. or agarose sections were used.

Paraffin sections were dewaxed in 100% xylene, rehydrated in a graded ethanol series and washed in PBS, and heat induced epitope retrieval (HIER) was performed with 0.01 M Sodium citrate (pH 6.0) before rinsed with PBS and PBT (1X PBS, 0.1% Triton X-100). Sections were blocked with 10% goat serum in PBT, incubated with primary antibody in PBT overnight at 4°C, washed six times at 30 min each in PBT, reblocked with 10% goat serum in PBT, incubated with Alexa Fluor secondary antibody used at 1:1000 from Life Technologies (Carlsbad, CA) for 2 hours at 25°C, and washed six times at 30min each in PBT.

Agarose and O.C.T. sections were washed in PBT, blocked with 10% goat serum in PBT, incubated with primary antibody in PBT overnight at 4°C, washed six times at 30 min each in PBT, reblocked with 10% goat serum in PBT, incubated with Alexa Fluor secondary antibody used at 1:1000 from Life Technologies (Carlsbad, CA) for 1 hours at 25°C, and washed six times at 30min each in PBT.

Primary antibodies used include: anti-Glutamine Synthetase at 1:500, anti-Laminin at 1:300, and anti-Calbindin-D-28K at 1:500 from Sigma-Aldrich (St. Louis, MO); anti-Rhodopsin at 1:200 from EMD Millipore (Billerica, MA); Xen1 at 1:100 and Islet-1 at 1:200 from the Developmental Studies Hybridoma Bank at the University of Iowa (Iowa City, IA). DAPI (4′,6-diamidino-2-phenylindole) from Life Technologies (Carlsbad, CA) was used as a DNA stain.

WHOLE-MOUNT IMMUNOHISTOCHEMISTRY

Tadpoles were fixed in MEMFA solution and antibody staining was performed as described previously (Sive et al., 2000). Primary antibodies used include: Xen1 at 1:50 from the Developmental Studies Hybridoma Bank at the University of Iowa (Iowa City, IA). Alexa Fluor secondary antibodies were used at 1:1000 from Life Technologies (Carlsbad, CA). TO-PRO®-3 (DNA stain) were used from ThermoFisher Scientific (Waltham, MA).

IMAGING WHOLE ANIMALS AND SECTIONS

Brightfield morphology of whole animals and H&E sections were imaged on a SteREO Discovery.V20 stereomicroscope (Zeiss). Whole-mount and tissue sectioned immunohistochemistry were imaged on a Nikon A1R confocal laser scanning microscope (Nikon) or on an Axio Imager 2 microscope (Zeiss). All acquired images were analyzed on either the ZEN Image Analysis software (Zeiss) or FIJI, an open-sourced imaging software (Schindelin et al., 2012).

STATISTICAL ANALYSIS

The raw data from scoring was used for the comparison of the eye regrowth experiments. Experiments with multiple treatments were compared using a Kruskal-Wallis test, with Dunn's Q corrected for tied ranks. All other experiments were analyzed using a Student's t-test.

CHAPTER 3

RESULTS

SURGICAL REMOVAL OF THE OPTIC VESICLE LED TO EYE REGENERATION

The Tseng lab developed an eye regeneration assay and observed that an eye can regeneration after eye organ removal from the tailbud embryo stage. With this result, the regenerate *Xenopus* tailbud embryo can be used as a new eye regeneration model. The eye regeneration assay protocol is described **(Figure 3)**. Tailbud embryos at development st. 27 were anesthetized and the optic vesicle tissue was surgically removed with Dumont No.5 forceps. Healing was observed after surgery and after five days of recovery, the surgical site show regeneration of an eye with similar phenotype to an eye of an unoperated control sibling with an RI= 286, total N= 86 **(Figure 4D, H)**. Brightfield images taken at the initial surgical day, 0 day post-surgery (dps), show the area with the removed optic vesicle tissue at 30 minutes after surgery where the wound has contracted after healing compared to an unoperated control **(Figure 4A, E)**. Eye tissues had regrown by 1 dps, but it was smaller in size compared to the control eye **(Figure 4B, F)**. By 2 dps, more tissue had regrown and the size differences were not as drastic **(Figure 4C, G)**. 5 dps showed the fast process of eye regeneration as there were no differences in eye size and morphology between most regenerated eye and control eye **(Figure 4D, H)**. Fully regenerated eyes were seen in 90.7% (N=78) of the total population (N=86), partial eye regeneration was seen in 4.7% (N=4), weak regeneration was seen in 3.5% (N=3), and no eye regenerated individuals were categorized as none in 1.2% (N=1) of the total population. Moreover, there was no developmental delay in the growth of the tadpoles.

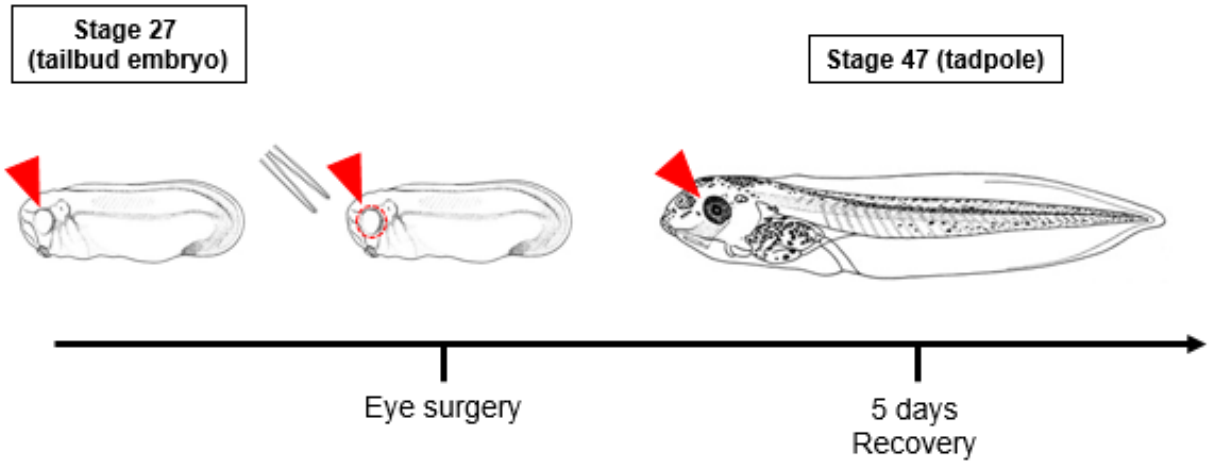

Figure 3. Eye regeneration assay. Surgical removal of one optic vesicle tissue at stage 27 tailbud embryo. Recovery and eye regrowth at surgical site observed for 5 days post-surgery until stage 47 tadpole. Closed arrowheads: surgical eye, red dotted line: surgical site.

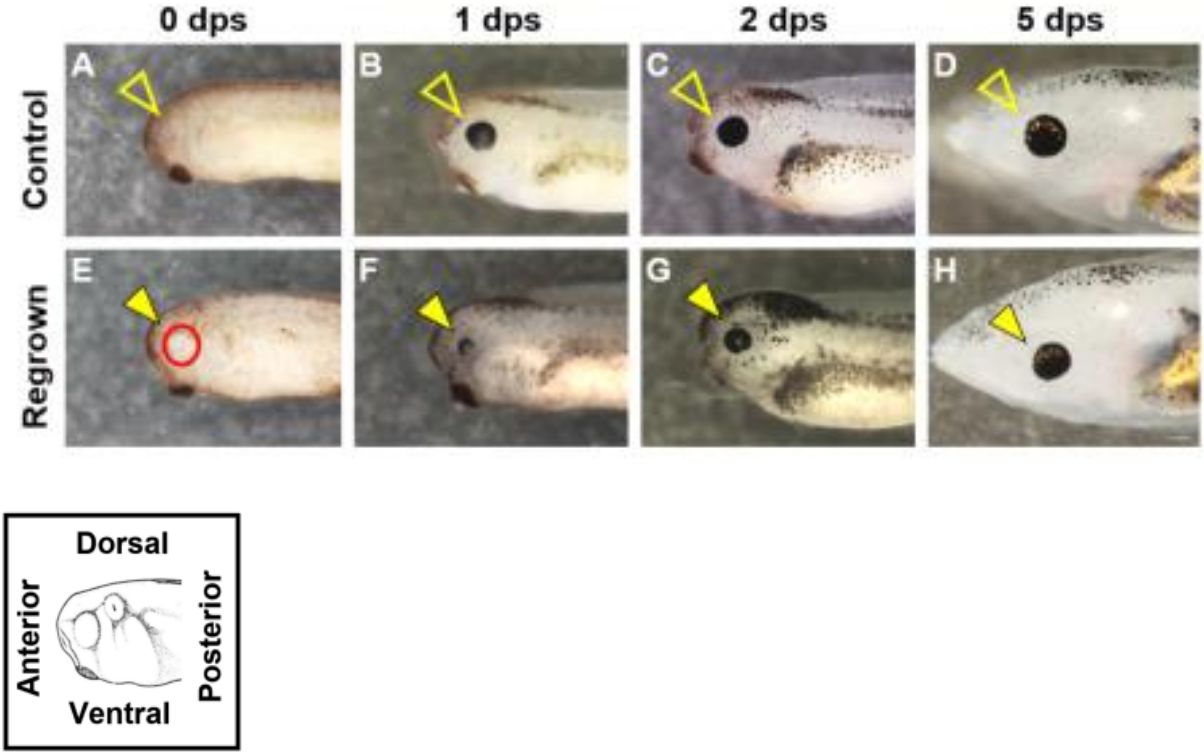

Figure 4. Regrowth of eye tissues after surgery compared to unoperated sibling eye. **(A-H)** Brightfield images show initial optic vesicle removal. **(A, E)** 30 minutes after surgery at 0 dps compared to a control eye. **(B, F)** 1 dps eye compared to control, **(C, G)** 2 dps eye compared to control, and **(D, H)** 5 dps eye compared to control. RI with full regeneration: 90.7% (N=78) of total population (N=86), partial regeneration: 4.7% (N=4), weak regeneration: 3.5% (N=3), none: 1.2% (N=1). Open arrowheads: unoperated control eye, closed arrowheads: surgical eye, red dotted line: surgical site. RI= 286. Scalebar= 200 µm.

BRAIN STRUCTURE IS UNAFFECTED DURING SURGERY

Having established that the eye regeneration assay can induce regeneration of an eye that is similar to the control eye, we wanted to show that the brain structure is unaffected during surgery. We took cross-sections of tailbud embryos at 0 dps after surgery **(Figure 5A)** and stained with hematoxylin and eosin (H&E) to show the undisturbed brain tissue present after optic vesicle tissue removal, N=11 **(Figure 5B, 5C)**. The brain structures appeared histologically normal and were present, compared to the cross-section schematic of a tailbud embryo, in contrast to the tissues removed at the surgical site. In addition, to establish the presence of the brain tissue, we performed a transverse section of the animal **(Figure 6A)**. Most optic vesicle tissue was removed at 0 dps and the neural tissues remained as identified with immunostainings, N=37 **(Figure 6B)**. Xen1 antibody was used to show the remaining neural tissues and control optic vesicle and anti-Laminin show the basal lamina to outline the brain tissue and optic vesicle. Minimal disruption was seen in the surrounding tissues compared to the tissues removed during surgery. We further quantified the amount of optic vesicle tissue removed during surgery. For each animal, the section containing the largest amount of eye tissues remaining after surgery was measured and compared to the area of the contralateral eye (internal control) to determine the percentage of tissue removed following surgery. The comparison between the measurements of the tissue remaining after surgery and the area of the contralateral eye were determined with a student's t-test. The eye regeneration assay show that during surgery, >95% of the area of the eye tissue was removed in 43.2% of tailbud embryos used in the eye regeneration assay, N=37 **(Figure 7)**.

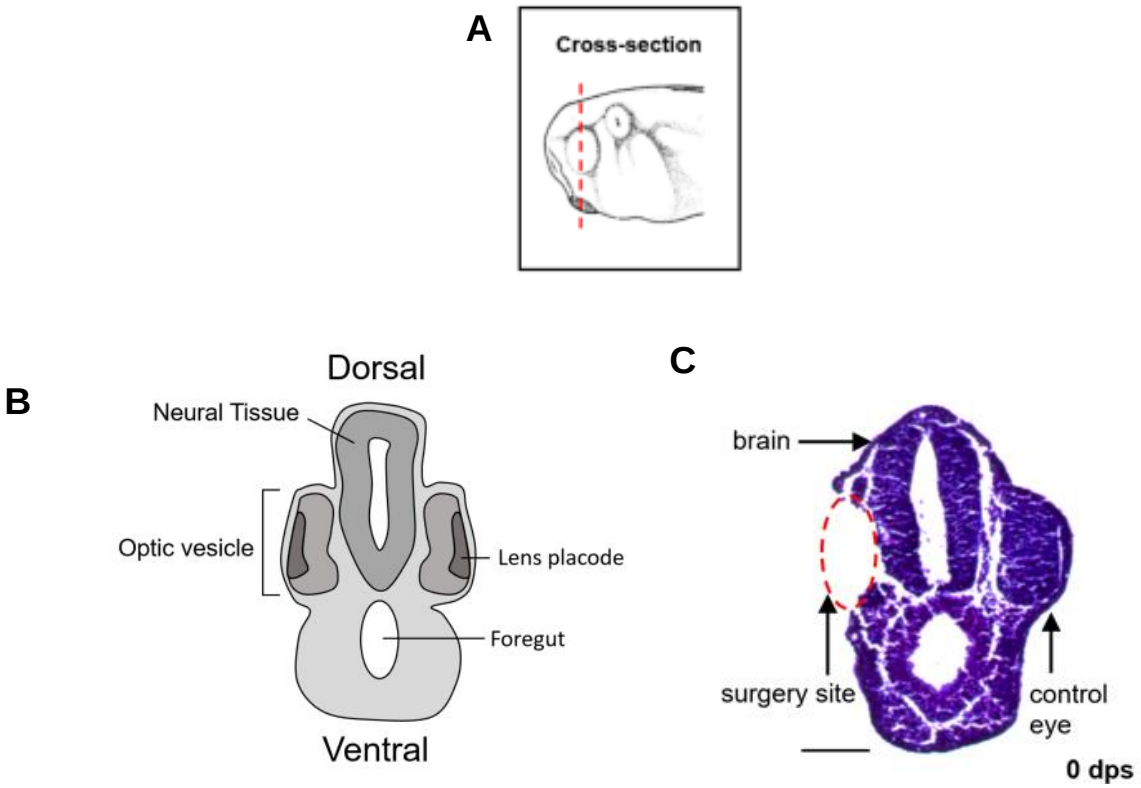

Figure 5. Hematoxylin and eosin staining (H&E) show eye tissue removed after surgery. **(A, B)** A cross-section of a stage 27 tailbud embryo show the location of the neural tissues flanked by the two optic vesicle showing the lens placode. Red dotted line: sections through the optic vesicle. **(C)** H&E section at 0 dps shows the removal of the optic vesicle after surgery leaving the neural tissues undisturbed. Red dotted line: surgical site. N= 11, scalebar= 100 µm.

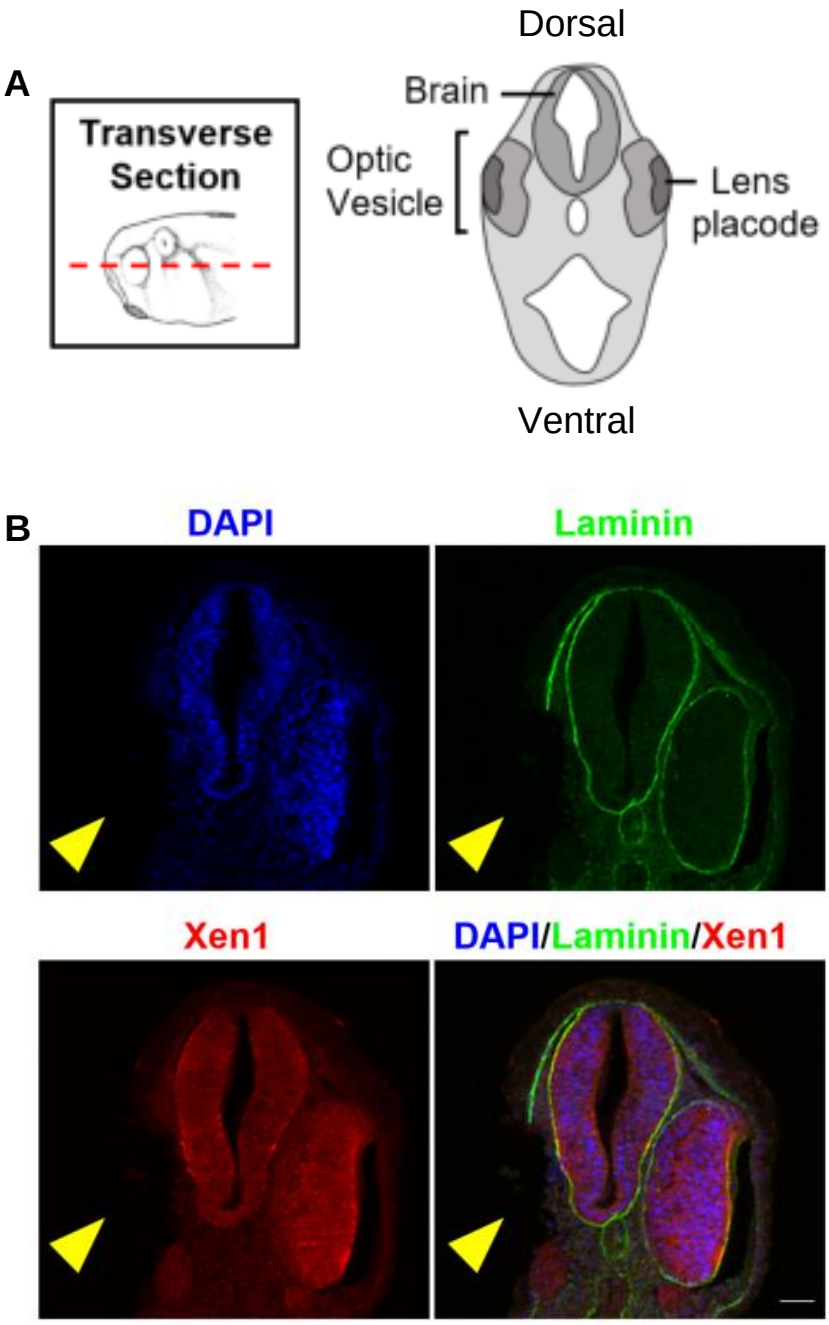

Figure 6. Immunostaining shows brain structure is unaffected during surgery. (**A)** Schematic of a transverse section through a st. 27 tailbud embryo. **(B)** Immunostained sections through the optic vesicle after surgery. Yellow arrowheads: surgical site. Blue: cell nuclei, green: basal lamina, red: pan-neural. N= 37, scalebar= 25 µm.

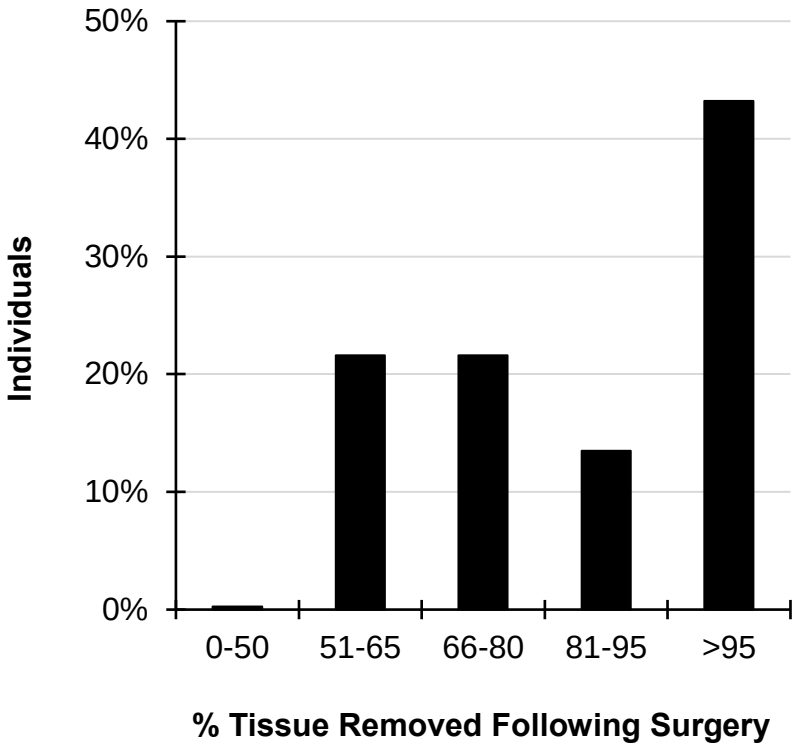

Score	Percentage
0-50	0
51-65	21.6
66-80	21.6
81-95	13.5
>95	43.2

Figure 7. Quantification of optic vesicle tissue removed during surgery. In 43.2% of tailbud embryos used for the eye regeneration assay, >95% of the optic vesicle tissue was removed following surgery. N=37.

SUFFICIENT EYE TISSUE IS REMOVED

We found that the eye regeneration assay can induce regeneration of the eye by five days of recovery, but we wanted to demonstrate sufficient tissue was surgically removed. To test this, we used a well-established eye transplantation assay (Blackiston and Levin, 2013) with modifications to remove eye tissues at the tailbud embryo stage **(Figure 8)**. Late tailbud embryos at developmental st. 27 were anesthetized and the optic vesicle tissue surgically removed with forceps. A small slit was placed in the same animal 1/3 from the posterior end of the body axis, in which the removed optic vesicle tissue was grafted. Following surgery at 0 dps, animals show wound healing by 30 minutes post-surgery **(Figure 9A)**. Wounds are healed by 1 dps and a regrown eye is present in the anterior head region **(Figure 9B)**. Additionally, a developing eye is seen in a raised pocket of epidermis along the trunk of the individual. By 5 dps, transplantation surgery induced an ectopic eye, N=6 **(Figure 9C)**. Generated ectopic developed at the same rate as the regenerating eye in the anterior head region. Additionally, the ectopic eye display similar morphology and mediolateral orientation to the regrown eye with a slightly smaller size. We noted no developmental differences in tissue grafted tadpoles compared to an unoperated control tadpole and no abnormal swimming behavior.

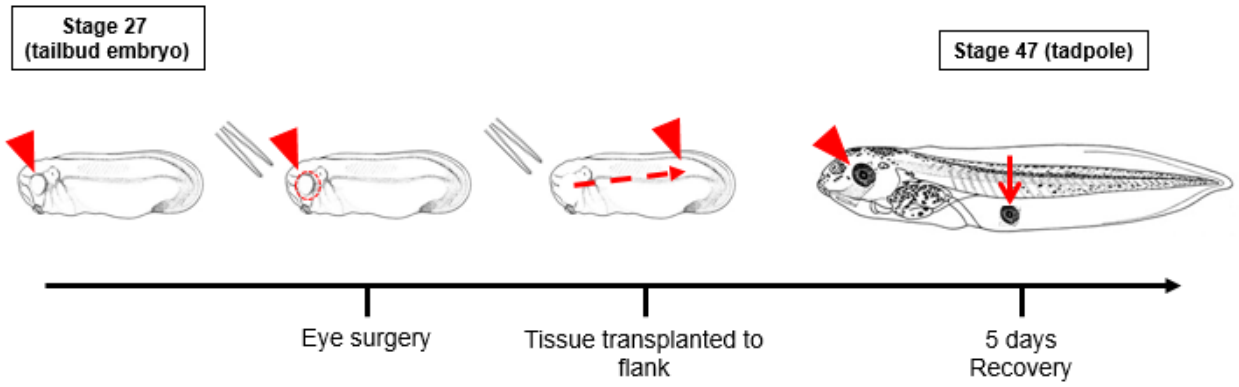

Figure 8. Eye transplant assay. Surgical removal of one optic vesicle at stage 27 tailbud embryo is transplanted to an incision in the flank, 1/3 from posterior end of body axis. Recovery and eye regrowth at surgical site and transplant site were observed for 5 dps until stage 47 tadpole. Closed arrowheads: surgical eye, dashed circle: surgical site; dashed line: transplant sites, arrow: ectopic eye at the transplant site.

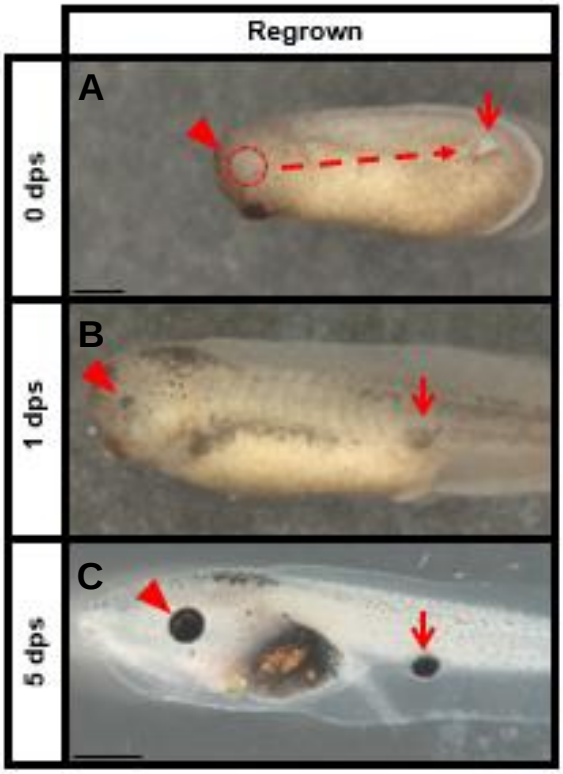

Figure 9. Regrowth of eye tissues and ectopic eye after transplant assay. (A) Brightfield image showing surgical removal of one optic vesicle at stage 27 tailbud embryo and transplanted to an incision in the posterior flank, 30 minutes after surgery at 0 dps. Closed arrowhead: surgical eye, dashed circle: surgical site, arrow: transplant site. Scalebar= 500 µm **(B)** 1 dps show tissue regrowth in both surgical and transplant sites. Closed arrowhead: surgical eye, arrow: ectopic eye. **(C)** 5 dps show no differences in eye morphology between regenerated eye in the anterior head region and ectopic eye in the flank. Closed arrowhead: surgical eye, arrow: ectopic eye. N= 6, scalebar= 500 µm.

REGENERATED EYE REGROWS ALL TISSUE STRUCTURES

Now that we knew sufficient optic vesicle tissue was removed, we investigated if the tissue removed can generate an eye with tissues layers similar to those in a human eye. We took cross-sections of tailbud embryos at 1 dps **(Figure 10A)** and stained with H&E to observe eye regeneration over a five day period **(Figure 10B-I)**. At 1 dps, there is a difference in size of the regrowing eye compared to the unoperated control sibling, N=7 **(Figure 10B, F)**. From 2 dps, the lens have developed and the retina further differentiates to form the distinctive retinal cell layers, but the regrown eye has not caught up to the size of the control eye, N= 5 **(Figure 10C, G).** At 3 dps, the eye has caught up in size comparable to the control eye, N=6 **(Figure 10D, H)**. By 5 dps, the regenerated eye is undisguisable in size and morphology to the control eye (**Figure 10E, I)** displaying the seven distinctive cell types and lens, N=5 **(Figure 10J)**.

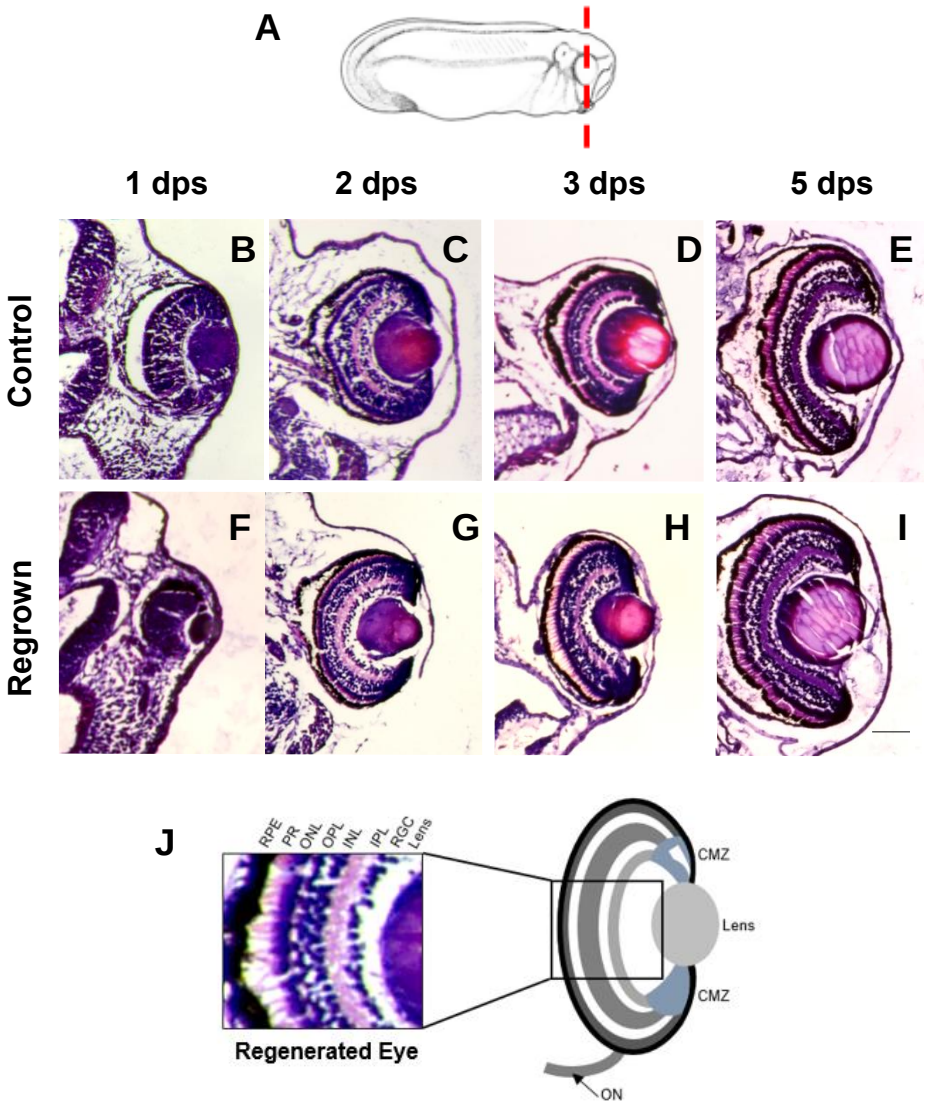

Figure 10. Regenerated eye regrows all tissue structures. (A) A schematic cross-section of a stage 27 tailbud embryo. Red dotted line: sections through the optic vesicle. **(B, F)** H&E section at 1 dps shows eye tissue growth at surgery site compare to the 1 day control eye. **(C-D, G-H)** 2 dps and 3 dps show differentiated eye tissues of the regrown eyes compared to the control eyes. **(E, I)** By 5 dps, a regenerated eye similar in tissue organization and size is apparent compared to the 5 day control eye. 1dps N= 7, 2 dps N= 5, 3 dps N= 6, 5 dps N=5, scalebar= 50 µm. **(J)** All seven layers of the retinal cells and the lens are present in the regenerated eye (schematic of regenerated eye adapted from Tseng, 2017).

To assess the presence and location of individual eye tissues, we performed immunostaining using different retinal cell markers on the regenerated eye as compared to the control eye at 5 dps. We used anti-Islet-1 antibody to label the ganglion cells and populations of amacrine, horizontal, and bipolar cells in the inner nuclear layer **(Figure 11)**. Anti-Rhodopsin and Anti-Calbindin-D-28K antibodies were used to label the rods and cones photoreceptors, respectively **(Figure 12)**. Anti-Glutamine Synthetase antibody was used to detect Müller glia cells **(Figure 13)**. Each of the retinal cells types tested were found in the regenerated eye in a similar pattern to that of the unoperated control eye. Brightfield images show the presence of the RPE. The presence of RGCs in the regenerated eye show that the GCL was re-established in the retina. Additionally, populations of the INL cells were distinguished by its location within the INL. The amacrine cells are located nearest to the GCL, bipolar cells in the middle, and bipolar cells located at the outermost edge of the GCL **(Figure 11)**. Also, the photoreceptor layer was re-established with the rods and cones located in a pattern similar to that of the control eye **(Figure 12)**. Furthermore, Müller glia cells were found extending vertically throughout the retina, with the nucleus residing in the middle of the INL **(Figure 13)**.

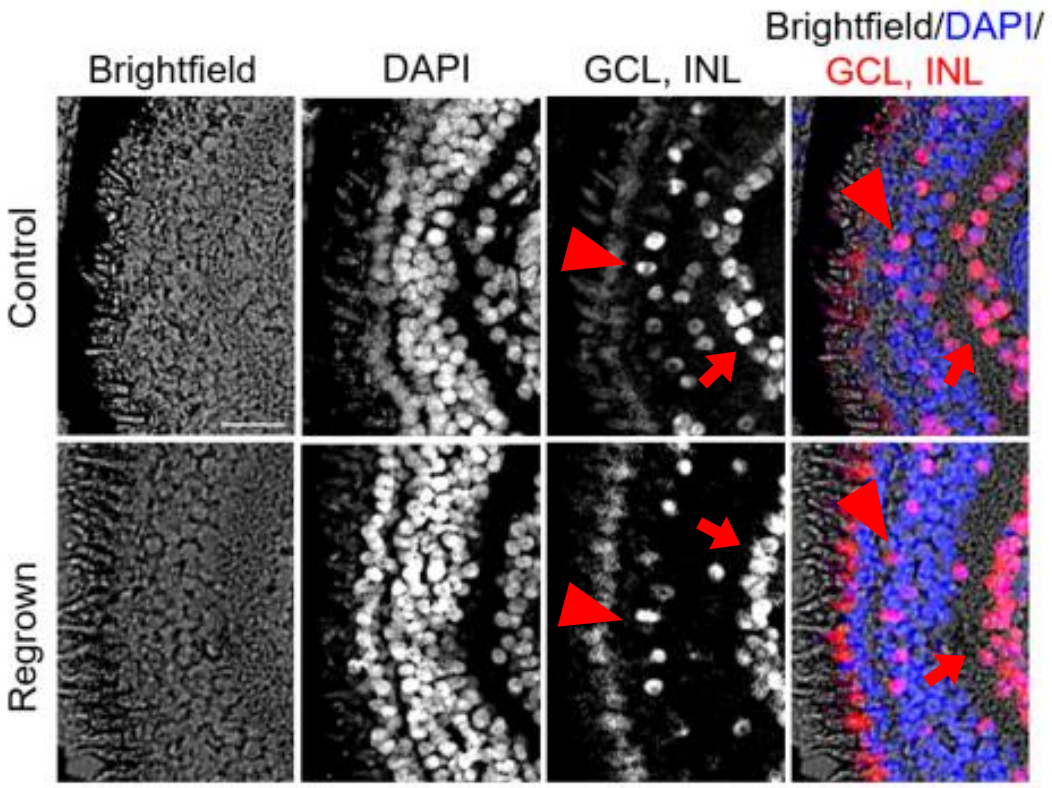

Figure 11. Regenerated eye at 5dps contains the ganglion cell layer and the inner nuclear layer. Different retinal cell types identified in eye regenerates comparable to the unoperated control eye. Closed arrowheads: INL display amacrine, bipolar, and horizontal cells. Arrows: GCL display retinal ganglion cells. Red: INL and GCL, Blue: cell nuclei. Scalebar= 50 µm.

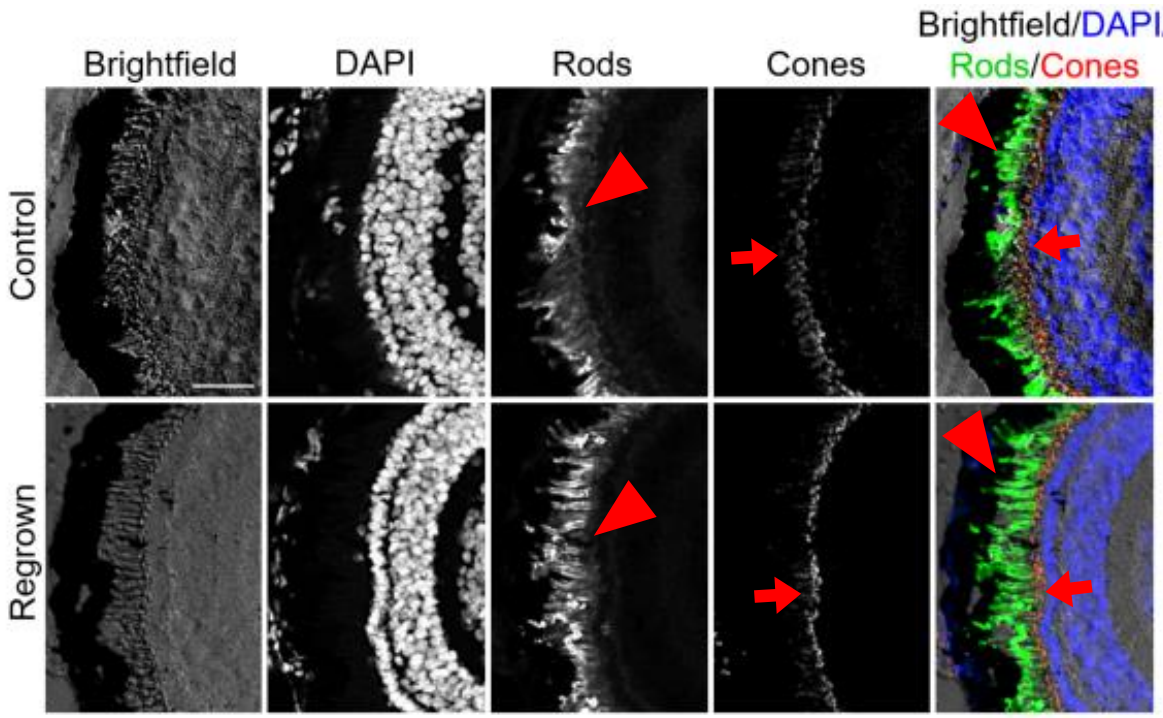

Figure 12. Regenerated eye has the photoreceptor layer present. Different retinal cell types identified in eye regenerates comparable to the unoperated control eye. Closed arrowheads: rod photoreceptors. Arrows: cone photoreceptors. Blue: cell nuclei, green: rods, red: cones. Scalebar= 50 µm.

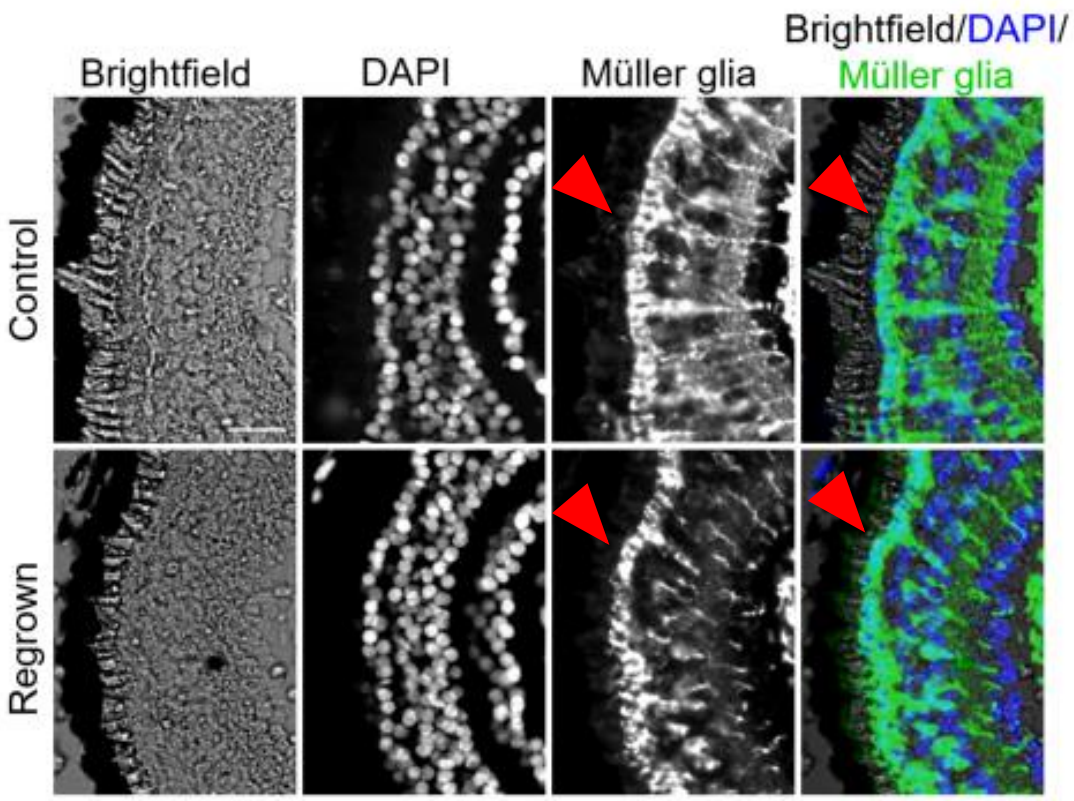

Figure 13. Regenerated eye Müller glial cells present. Different retinal cell types identified in eye regenerates comparable to the unoperated control eye. Closed arrowheads: Müller glial cells. Blue: cell nuclei, green: Müller glial cells. Scalebar= 50 µm.

V-ATPASE IS MECHANISM FOR REGULATING EYE REGENERATION

To address if the mechanism used in appendage regeneration is an organ-specific mechanism or is also found in eye regeneration, we performed a loss-of-function assay **(Figure 14)**. The left optic vesicle tissue was removed from late tailbud embryos at development st. 27. Immediately after surgery, the individuals were placed in a petri dish with a V-ATPase chemical inhibitor, concanamycin at 20 nM for one day and then washed with 0.1X MMR. The potent and highly specific chemical, concanamycin, was used to inhibit the function V-ATPase H^+ proton pump (Woo et al., 1996). We observed normal wound healing phenotype and block of eye regeneration by 1 dps (N= 6) when compared to an unoperated control sibling (N= 3) and a surgical sibling that was treated with only DMSO (N= 3) **(Figure 15A)**. Furthermore, H&E histological cross-sections showed no regrowth of eye tissues by 1dps (N=6) compared the DMSO control group (N=4) **(Figure 15B)**. The exposure to 20 nM concanamycin showed strong inhibition of eye regeneration by 5 dps, as the most severe phenotype, N= 5 **(Figure 16A)**. Also observed was the absence of toxicity or developmental delays or abnormalities in the treated tadpoles compared to the untreated siblings (N=40). An immunostaining with Xen1 for neural tissue further show no eye tissue and optic nerve formation five days after recovery, N=3 **(Figure 16B)**. We further quantified the extent of inhibition on eye regeneration based on our eye regeneration efficiency score and saw a significant block of eye regeneration as our most severe phenotype **(Figure 17).** The 20 nM concanamycin treated group had eye regeneration seen in 50.3% of individuals and an RI of 151 (N=23), compared to the DMSO control group with eye regeneration seen in 94.8% of individuals and an RI of 287.5 (N= 27); Kruskal-Wallis test followed with Dunn's Q show a value of significance at $*P<0.01$. Other dosages of the chemical were tested and a dose-dependent effect was seen (data not shown).

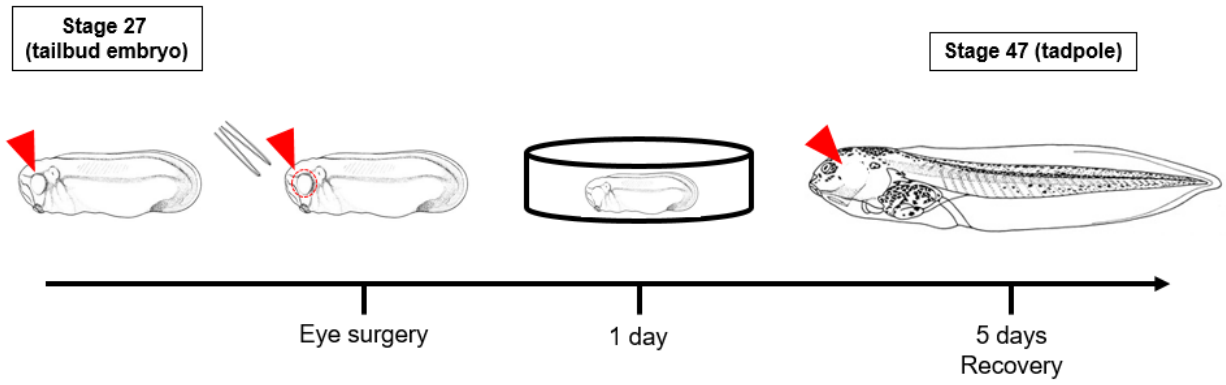

Figure 14. Functional assay to test inhibitors on eye regeneration. Surgical removal of one optic vesicle at stage 27 tailbud embryo. Immediately after surgery, animals are exposed to 20 nM concanamycin in a petri dish for one day. 5 days after recovery, eye regeneration efficiency was scored. Closed arrowheads: surgical eye, dashed circle: surgical site.

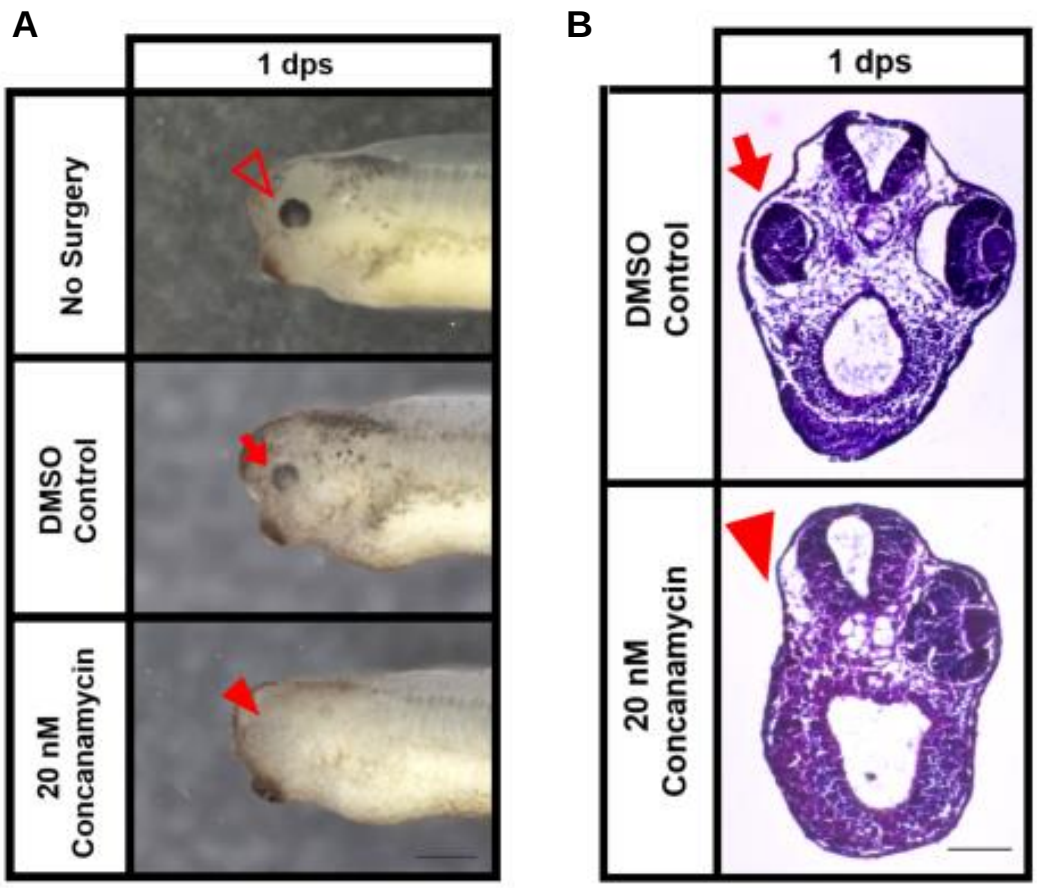

Figure 15. Inhibition of V-ATPase activity blocks eye regeneration by 1 day. (A) Brightfield image show inhibition of eye regeneration in the treatment group compared to a surgical sibling with no inhibitor exposure and an unoperated control sibling. Open arrowhead: unoperated eye, arrow: surgical eye with no inhibitor exposure, closed arrowhead: surgical eye with 20 nM concanamycin treatment. No surgery controls N=3, DMSO treated controls N=3, 20 nM concanamycin treated N= 6, scalebar= 500 µm. **(B)** H&E section at 1 dps shows no eye tissue regrowth after 20 nM concanamycin exposure in comparison to a regenerating eye in an untreated sibling exposed to DMSO. Arrow: surgical eye control exposed to DMSO. Closed arrowhead: surgical site with 20 nM concanamycin exposure. N=4, scalebar= 100 µm.

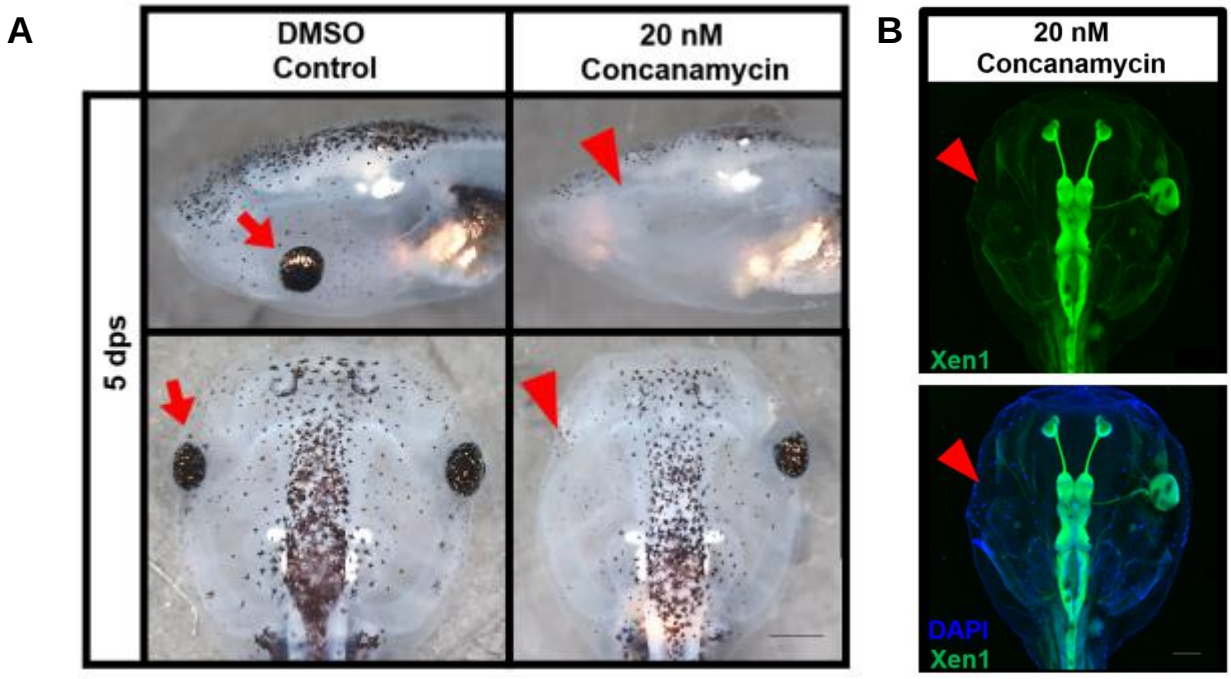

Figure 16. Inhibition of V-ATPase activity blocks eye regeneration 5 days after recovery. **(A)** Brightfield image at 5 dps show inhibition of eye regeneration in a tadpole exposed to 20 nM concanamycin compared to a regenerating eye in a control, untreated tadpole exposure to DMSO. Arrow: surgical eye, closed arrowhead: surgical site. DMSO treated controls N=27, 20 nM concanamycin treated N=5, scalebar= 500 µm. **(B)** Immunostained sections through the eye of a tadpole after exposure to 20 nM concanamycin show no presence of eye tissue and an optic nerve. Closed arrowheads: surgical site. Blue: cell nuclei, green: pan-neural. N= 3, scalebar= 200 µm.

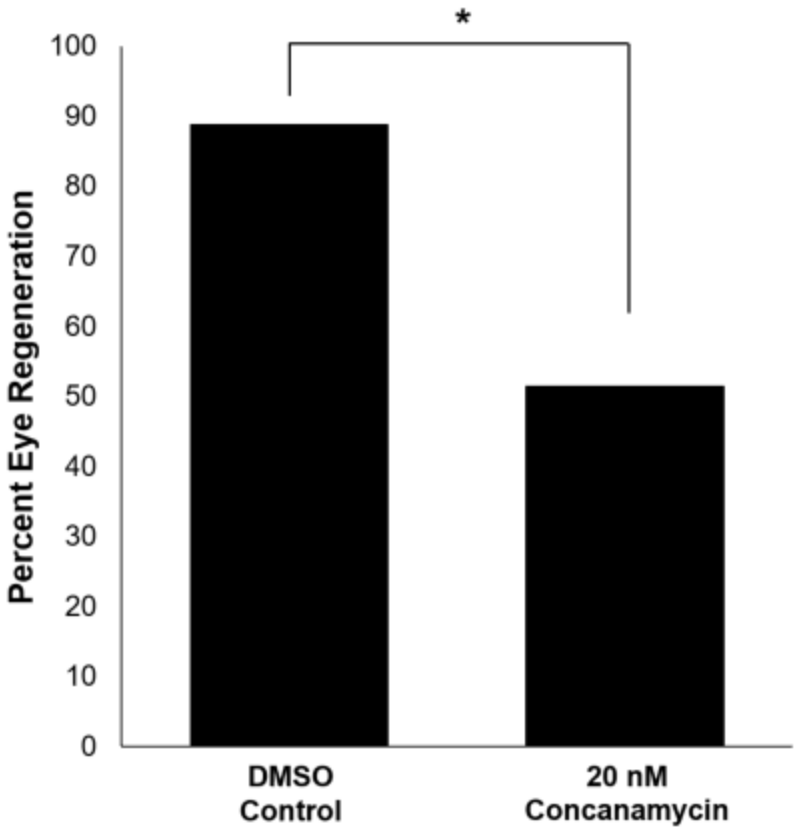

Figure 17. Quantification of inhibition of V-ATPase activity on eye regeneration. Percentage of eye regeneration in a DMSO control group compared to eye regeneration in a group after exposure to 20 nM concanamycin. Inhibitor treated group had eye regeneration seen in 50.3% of individuals (RI of 151) compared to the DMSO control group with eye regeneration seen in 94.8% of individuals (RI of 287.5). DMSO control: N=27, 20 nM concanamycin treated: N=23. Eye regeneration efficiency evaluated with a Kruskal-Wallis followed by Dunn's Q, *$P<0.01$.

WINDOW ALLOWING EYE REGENERATION

Our results show that following one optic vesicle tissue removal of a tailbud embryo, eye regeneration occurred. However, it was previously found that removal of an eye field during neurulation or removal of an eye during the tadpole stage does not allow this ability (Zuber, 2010; Blackiston et al., 2013). Given these results, we knew that a tailbud embryo can regenerate an eye so a competency window for eye regeneration must exist. To find the window that allows for regeneration, we performed the eye regeneration assay from the tailbud embryo stages to the early tadpole stages **(Figure 18)**. The stages are as follows: st. 26 (RI= 272, N= 25); st. 27 (RI= 277.9, N= 882); st. 28 (RI= 242.1, N= 57); st. 29-30 (RI= 173.1, N=83); st. 31 (RI= 171.4, N=72); st. 32 (RI= 112.3, N= 77); st. 33-34 (RI= 41.6, N= 82); st. 35-36 (RI= 19.8, N=74); st. 37-38 (RI= 0, N= 30); st. 39 (RI= 0, N=33); st. 40 (RI= 0, N=35). We found that a window for eye regeneration exists, but there was a decreased in regenerative potential with further eye specification.

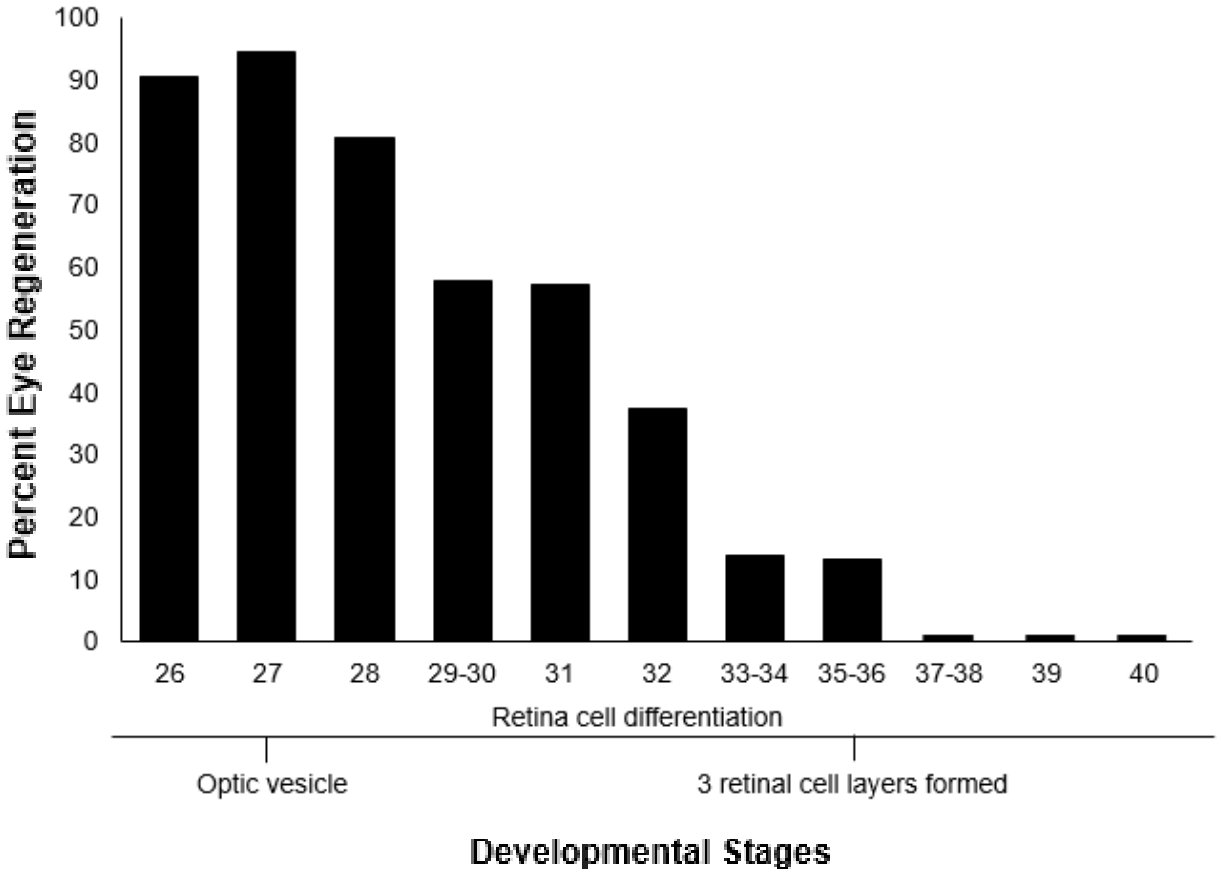

Figure 18. Developmental window allowing eye regeneration. Percentage of eye regeneration in tailbud embryos through early tadpoles with further retina cell differentiation. Stages of developmental subjected to the eye regeneration assay are as follows: st. 26 (RI= 272, N= 25); st. 27 (RI= 277.9, N= 882); st. 28 (RI= 242.1, N= 57); st. 29-30 (RI= 173.1, N=83); st. 31 (RI= 171.4, N=72); st. 32 (RI= 112.3, N= 77); st. 33-34 (RI= 41.6, N= 82); st. 35-36 (RI= 19.8, N=74); st. 37-38 (RI= 0, N= 30); st. 39 (RI= 0, N=33); st. 40 (RI= 0, N=35).

CHAPTER 4

CONCLUSIONS

The *Xenopus* frog has been widely used in developmental biology and provides many advantages as a model for research. Many molecular and genetic tools are available for use in the *Xenopus* model. This includes the abilities for targeted gene knock-out, knockdown, and overexpression studies. However, the potential for the multi-tissue eye organ regeneration research has not been fully evaluated, with much research dealing with eye tissue regeneration focused on individual eye tissue components, such as the retina in later stage tadpoles (Vergara and Rio-Tsonis, 2009).

In this study, a model for eye regeneration following surgical removal of the optic vesicle tissue, using *X. laevis* tailbud embryos is established. We observed high capacity for eye regeneration, generating a complete retina and lens, *in vivo* during a specific development window where the eye tissues are already specified and have started to differentiate. We showed that missing optic vesicles could regenerate an eye undisguisable from a normal development eye in phenotype, orientation, and size. We used histological and molecular markers to characterize the regenerated tissues and found all the differentiated cell types presence in normal pattern that constitutes a retina. This suggests that removal of most optic vesicle tissue does not change the proper differentiation and patterning of the retina during the regeneration process. Our regeneration assay demonstrated that most of the optic vesicle tissue was removed during surgery, but this does not discard the possibility that the remaining RPE is still able participate to regenerate the retina (Vergara and Rio-Tsonis, 2009; Yoshii et al., 2007).

In a developing visual system of *X. laevis*, RGCs project axons out from the eye to the brain to convey visual information (Rigel and Lom, 2004). The presence of RGCs in the regenerated eye shows that the GCL was re-established in the retina and may suggest the possibility of a developed optic nerve. Our previous lab technician, Julia Lauper, observed that the regenerated eye can innervate to the brain through the presence of the optic nerve. To determine if the regenerated eye confers vision to the tadpole, a previously described visual preference assay was performed by our undergraduate student, Hyunbae Son (Viczian et al., 2014). The initial data demonstrated tadpoles with regenerated eye behaved similar to an unoperated control sibling suggesting normal visual function was established.

In previous research, the modulation of a bioelectrical event, such as the initiation of intracellular sodium through voltage-gated sodium channels, is important for tail regeneration (Tseng et al., 2010). The flux of H+ ion flow driven by the V-ATPase pump caused changes to membrane voltage potential that are necessary to initiation tail regeneration. Given the importance of the V-ATPase pump to initiate tail regeneration, we wanted to address if this mechanism is organ specific during a tail regeneration event or if it has a role in eye organ regeneration. My work suggests that V-ATPase activity contributes to the regeneration specific H+ ion flux allowing the eye regeneration program initiate. This finding is significant as it might provide a generate mechanism for regeneration across all organ systems. Moreover, the ability to manipulate this mechanism can potentially initiate a regeneration event to occur even in cases where regeneration is limited.

Overall, our work provides a model for multi-tissue eye regeneration. The inherent ability of the *Xenopus* eye to regenerate may lead to the possibility of manipulating the *Xenopus* eye at older development stages into entering a regenerative state. In additional, it may be

possible to identify the signaling pathways that are involved during regeneration. Furthermore, if these signaling pathways are found to be evolutionarily conserved, it may lead to future regeneration work on other organ systems or animals.

REFERENCES

Araki, M. (2014). *A model for retinal regeneration in Xenopus*. In: M. Kloc, J. Z. Kubiak (Eds.), *Xenopus Development* (pp. 346–367). Oxford, New York. doi:10.1002/9781118492833.ch18

Beck, C. W., Christen, B., & Slack, J. M. (2003). Molecular Pathways Needed for Regeneration of Spinal Cord and Muscle in a Vertebrate. *Developmental Cell,5*(3), 429-439. doi:10.1016/s1534-5807(03)00233-8

Blackiston, D. J., & Levin, M. (2013). Ectopic eyes outside the head in Xenopus tadpoles provide sensory data for light-mediated learning. *Journal of Experimental Biology,216*(6), 1031-1040. doi:10.1242/jeb.074963

Choi, R. Y., Engbretson, G. A., Solessio, E. C., Jones, G. A., Coughlin, A., Aleksic, I., … Zuber, M. E. (2011). Cone degeneration following rod ablation in a reversible model of retinal degeneration. *Investigative Ophthalmology & Visual Science*, 52, 364–373. doi:10.1167/iovs.10-5347

Chow, R. L., & Lang, R. A. (2001). Early Eye Development in Vertebrates. *Annual Review of Cell and Developmental Biology,17*(1), 255-296. doi:10.1146/annurev.cellbio.17.1.255

Eguchi, G., Eguchi, Y., Nakamura, K., Yadav, M. C., Millán, J. L., & Tsonis, P. A. (2011). Regenerative capacity in newts is not altered by repeated regeneration and ageing. *Nature Communications,2*, 384. doi:10.1038/ncomms1389

Filoni, S. (2009). Retina and lens regeneration in anuran amphibians. *Seminars in Cell & Developmental Biology*, 20, 528–534. doi:10.1016/j.semcdb.2008.11.015

Freeman, G. (1963). Lens regeneration from the cornea in *Xenopus laevis*. *Journal of Experimental Zoology*, 154, 39–65.

Henry, J. J., & Grainger, R. M. (1990). Early tissue interactions leading to embryonic lens formation in Xenopus laevis. *Developmental Biology,141*(1), 149-163. doi:10.1016/0012-1606(90)90110-5

Hidalgo, M., Locker, M., Chesneau, A., & Perron, M. (2014). Stem cells and regeneration in the *Xenopus*retina. In: *Regenerative Biology of the Eye*, *Stem Cell Biology & Regenerative Medicine* (pp. 83–99). New York, NY: Springer. doi:10.1007/978-1-4939-0787-8_4

Hollyfield, J. G. (1971). Differential growth of the neural retina in *Xenopus laevis* larvae. *Developmental Biology*, 24, 264–286.

Ide, C. F. (1988). Role of cell displacement, cell division, and fragment size in pattern formation during embryonic retinal regeneration in Xenopus. *Acta Biologica Hungarica*, 39, 179–189.

Lin, G., Chen, Y., & Slack, J. (2013). Imparting Regenerative Capacity to Limbs by Progenitor Cell Transplantation. *Developmental Cell*,*24*(1), 41-51. doi:10.1016/j.devcel.2012.11.017

Martinez-De Luna, R. I., & Zuber, M. E. (2014). Putting regeneration into regenerative medicine. *Journal of Ophthalmic & Visual Research*, 9, 126–133.

McAvoy, J. W., & Dixon, K. E. (1977). Cell proliferation and renewal in the small intestinal epithelium of metamorphosing and adult *Xenopus laevis*. *Journal of Experimental Zoology*,*202*(1), 129-137. doi:10.1002/jez.1402020115

Mitashov, V. I., & Maliovanova, S. D. (1981). Cellular proliferative potentials of the pigment and ciliated epithelium of the eye in clawed toads normally and during regeneration. *Ontogenez*, 13, 228–234.

Nieuwkoop, P. D., & Faber, J. (1994). *Normal table of Xenopus laevis (Daudin): a systematical and chronological survey of the development from the fertilized egg till the end of metamorphosis*. New York: Garland.

Oberpriller, J. O., & Oberpriller, J. C. (1974). Response of the adult newt ventricle to injury. *Journal of Experimental Zoology*,*187*(2), 249-259. doi:10.1002/jez.1401870208

Parker, F., Robbins, S. L., & Loveridge, A. (1947). Breeding, Rearing and Care of the South African Clawed Frog (Xenopus laevis). *The American Naturalist,81*(796), 38-49. doi:10.1086/281498

Reeve, J. G., & Wild, A. E. (1978). Lens regeneration from cornea of larval *Xenopus laevis*. *Journal of Embryology and Experimental Morphology,* 48, 205–214

Reh, T. A. (1989). The Regulation of Neuronal Production during Retinal Neurogenesis. *Development of the Vertebrate Retina,* 43-67. doi:10.1007/978-1-4684-5592-2_3

Rigel, R., Lom, B. (2004) *Xenopus laevis* Retinal Ganglion Cell Dendritic Arbors Develop Independently of Visual Stimulation. *Impulse: The Premier Journal for Undergraduate Publications in the Neurosciences, 1*(1), 1–58.

Schindelin, J., Arganda-Carreras, I., Frise, E., Kaynig, V., Longair, M., Pietzsch, T., Cardona, A. (2012). Fiji: an open-source platform for biological-image analysis. *Nature Methods,9*(7), 676-682. doi:10.1038/nmeth.2019

Session, A. M., Uno, Y., Kwon, T., Chapman, J. A., Toyoda, A., Takahashi, S., Rokhsar, D. S. (2016). Genome evolution in the allotetraploid frog *Xenopus laevis*. *Nature*, 538, 336–343. doi:10.1038/nature19840

Sive, H. L., Grainger, R. M., & Harland, R. M. 2010. *Early development of Xenopus laevis: A laboratory manual*. Cold Spring Harbor, New York: Cold Spring Harbor Laboratory Press.

Spallanzani L. 1768. *Prodromo di un opera da imprimersi sopra la riproduzioni anamali*. Giovanni Montanari, Modena. Translated in English by Maty M. 1769. An essay on animal reproduction. London: T. Becket & DeHondt.

Tseng, A. (2017). Seeing the future: using Xenopus to understand eye regeneration. *Genesis,55*(1-2). doi:10.1002/dvg.23003

Tseng, A., Beane, W. S., Lemire, J. M., Masi, A., & Levin, M. (2010). Induction of Vertebrate Regeneration by a Transient Sodium Current. *Journal of Neuroscience,30*(39), 13192-13200. doi:10.1523/jneurosci.3315-10.2010

Vergara, M.N., Del Rio-Tsonis, K. (2009). Retinal regeneration in the *Xenopus laevis* tadpole: a new model system. *Molecular Vision*, *15*,1000–1013

Viczian, A. S., & Zuber, M. E. (2014). A Simple Behavioral Assay for Testing Visual Function in *Xenopus laevis*. *Journal of Visualized Experiments,* (88). doi:10.3791/51726

Wallingford, J. B. (2010). Preparation of Fixed Xenopus Embryos for Confocal Imaging. *Cold Spring Harbor Protocols,2010*(5). doi:10.1101/pdb.prot5426

Wan, J., & Goldman, D. (2016). Retina regeneration in zebrafish. *Current Opinion in Genetics & Development*, 40, 41–47. doi:10.1016/j.gde.2016.05.009

Wetts, R., & Fraser, S. E. (1988). Multipotent precursors can give rise to all major cell types of the frog retina. *Science*, 239, 1142–1145.Zuber, M. E. (2010). Eye field specification in *Xenopus laevis*. *Current Topics in Developmental Biology*, 93, 29–60. doi:10.1016/B978-0-12-385044-7.00002-3

Wetts, R., Serbedzija, G. N., & Fraser, S. E. (1989). Cell lineage analysis reveals multipotent precursors in the ciliary margin of the frog retina. *Developmental Biology*, 136, 254–263. doi:10.1016/0012-1606(89)90146-2

Woo, J., Ohba, Y., Tagami, K., Sumitani, K., Yamaguchi, K., & Tsuji, T. (1996). Concanamycin B, a Vacuolar H -ATPase Specific Inhibitor Suppresses Bone Resorption in Vitro. *Biological & Pharmaceutical Bulletin*,*19*(2), 297-299. doi:10.1248/bpb.19.297

Yoshii, C., Ueda, Y., Okamoto, M., & Araki, M. (2007). Neural retinal regeneration in the anuran amphibian *Xenopus laevis* post-metamorphosis: Transdifferentiation of retinal pigmented epithelium regenerates the neural retina. *Developmental Biology*, 303, 45–56. doi:10.1016/j.ydbio.2006.11.024

Zuber, M. E. (2010). Eye field specification in *Xenopus laevis*. *Current Topics in Developmental Biology*, 93, 29–60. doi:10.1016/B978-0-12-385044-7.00002-3

Zuber, M. E., Gestri, G., Viczian, A. S., Barsacchi, G., & Harris, W. A. (2003). Specification of the vertebrate eye by a network of eye field transcription factors. *Development*, 130, 5155–5167. doi:10.1242/dev.00723

CURRICULUM VITAE

Cindy X. Kha

Email: kha@unlv.nevada.edu

Education:

Bachelor of Science – Neuroscience
University of California, Riverside
2010

Master of Science – Biology
California State University, Los Angeles
2014